*Electronic Supporting Information (ESI)*

*for*

# Zn Capped $Al_2O_3$ and $TiO_2$ Nanoporous Arrays as pH-Sensitive Drug Delivery Systems: A Combined Experimental and Simulation Study

Rokhsareh Khodabandeh,[a] Fatemeh Mohammadpour,[b,*] Amin Reza Zolghadr,[a,*] and Axel Klein[a,c*]

a Department of Chemistry, Shiraz University, Shiraz, 71946-84795, Iran
[b] Department of Physics, Farhangian University, Tehran, Iran
[c] Department für Chemie, Institut für Anorganische Chemie, Universität zu Köln, Greinstraße 6, D-50939 Köln, Germany

[*]Corresponding authors: f.mohammadpour60@gmail.com (F.M); *arzolghadr@shirazu.ac.ir;* Tel: +98 713 613 7157, Fax: +98 713 646 0788, ORCID: 0000-0002-6289-3794 (A.R.Z); axel.klein@uni-koeln.de; Tel.: +49-221-470-4006, ORCID: 0000-0003-0093-9619 (A.K.)

## Contents

## A) Supporting Figures

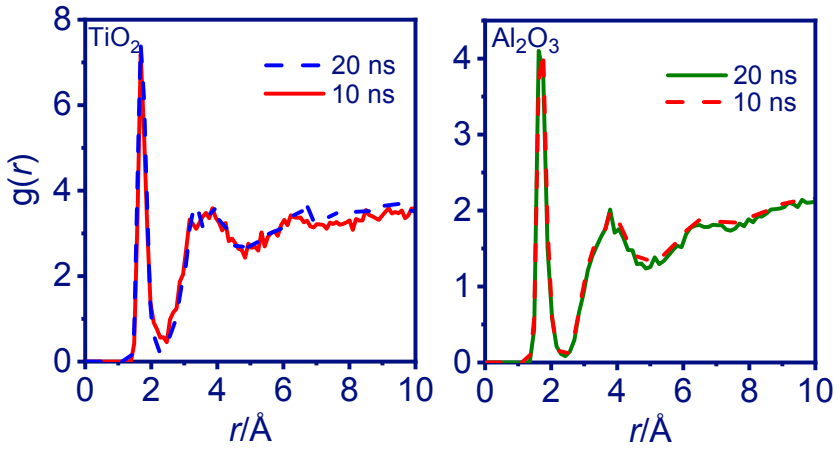


**Fig. S1** Radial distribution functions g(*r*) of vitamin C with water confined inside the $Al_2O_3$ and $TiO_2$ nanopores at different simulation times.

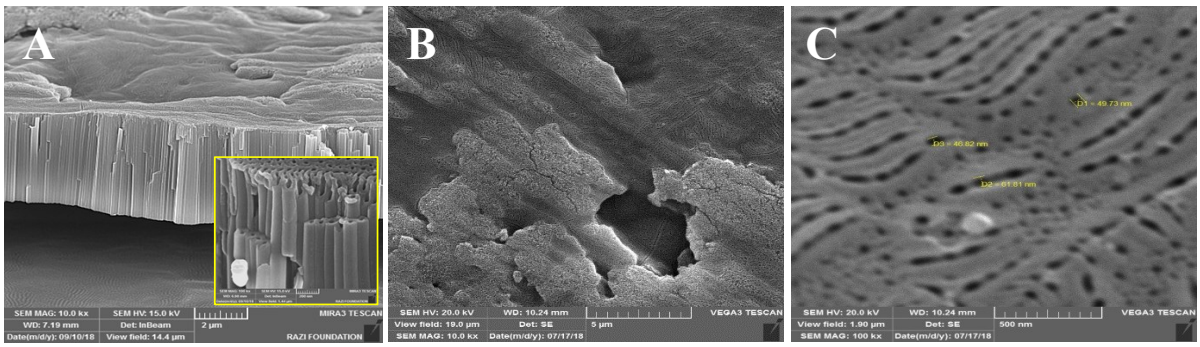


**Fig. S2** SEM images of $TiO_2$(40nm) nanoporous arrays from potentiostatic anodisation, cross-section (A) and top views in low magnification (B) and high magnification (C).

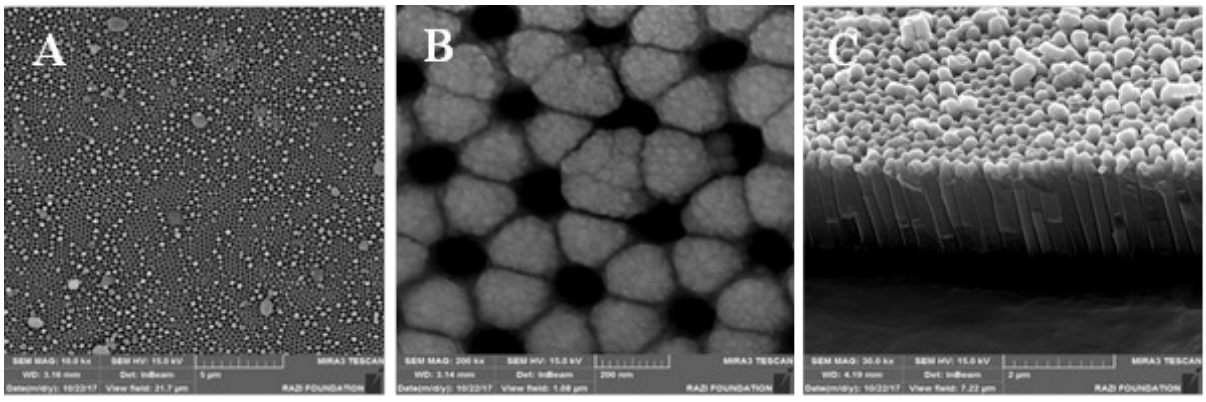


**Fig. S3** SEM images of Zn sputtered $Al_2O_3$(100nm) nanoporous arrays, top-view (A, B) and cross-section (C).

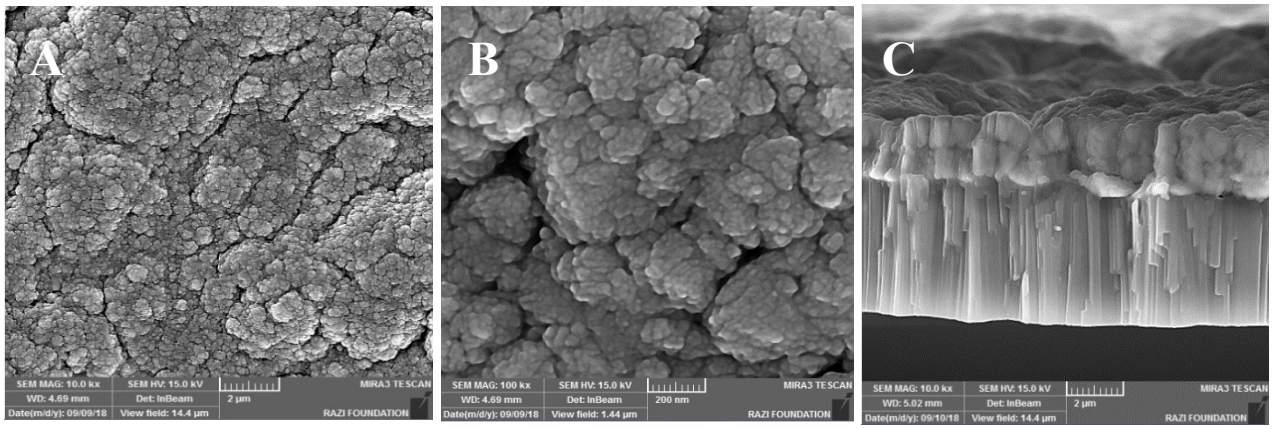


**Fig. S4** SEM images of Zn sputtered $TiO_2$(40nm) nanoporous arrays from the potentiostatic anodisation method, top view (A, B) and cross-section (C).

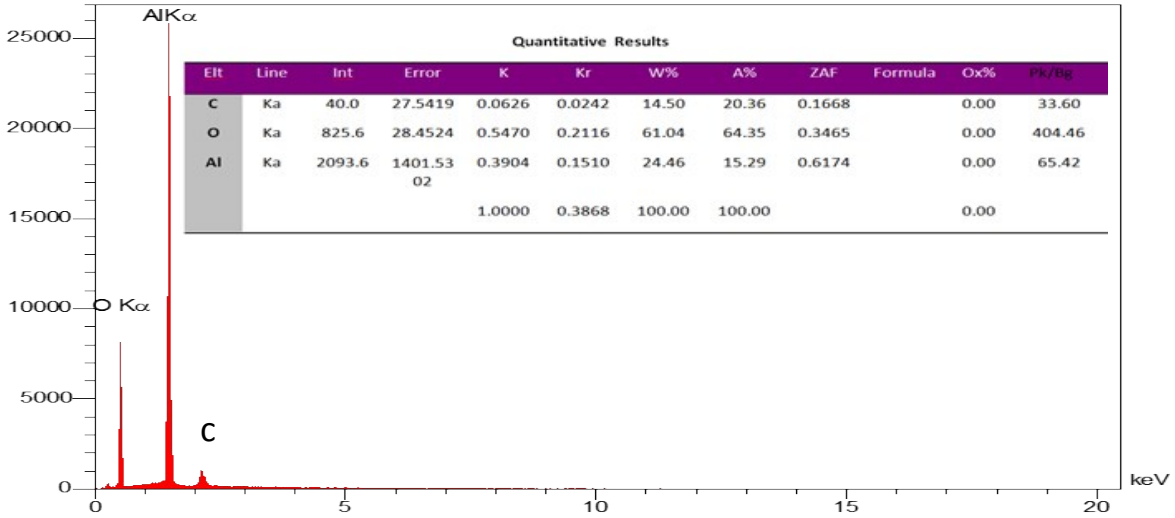


**Fig. S5** EDX spectrum and quantitative data (inset) of vitamin C loaded $Al_2O_3$(40nm) nanoporous arrays.

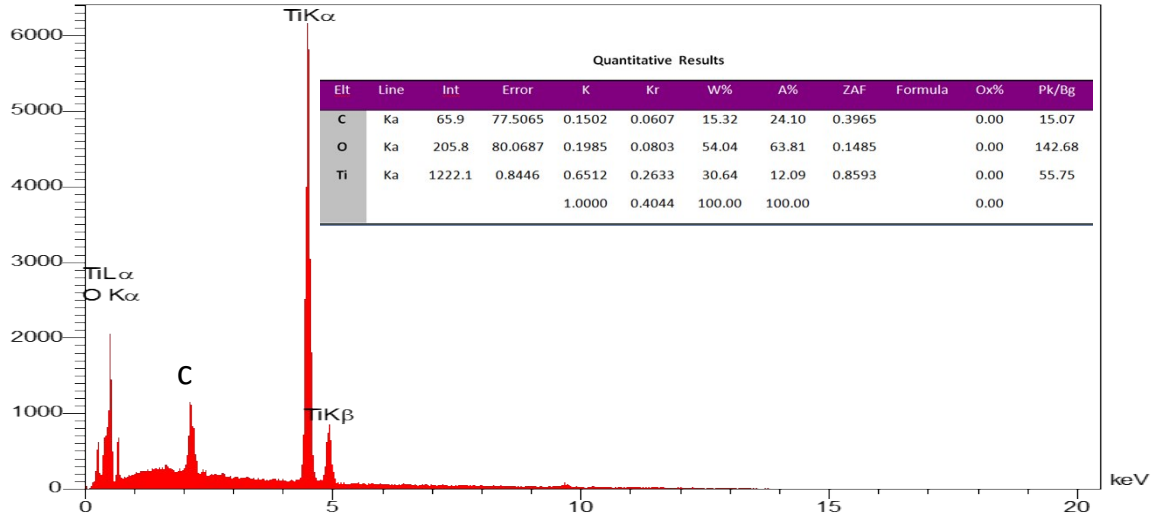


**Fig. S6** EDX spectrum and quantitative data (inset) of vitamin C loaded $TiO_2$(40nm) nanoporous arrays.

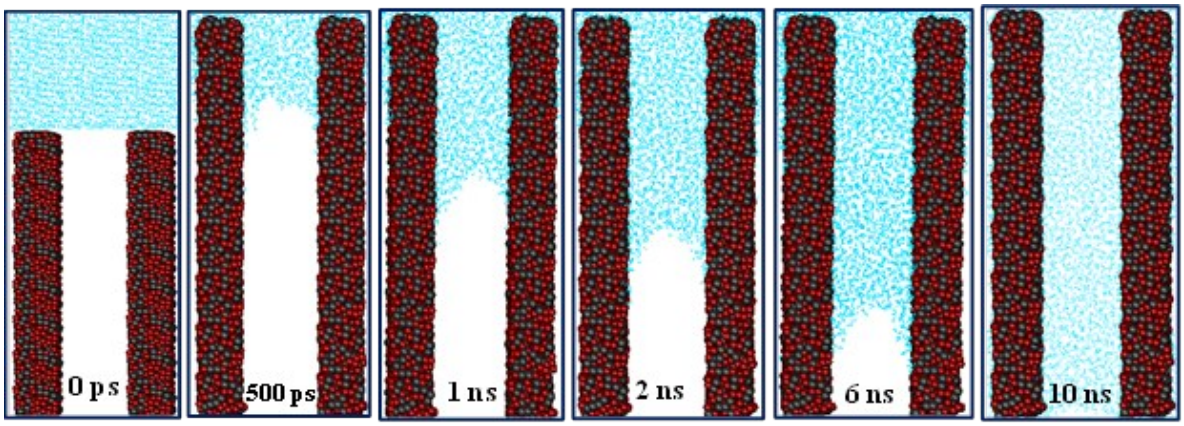


**Fig. S7** Representative MD simulation snapshots of water loading into a $Al_2O_3$ nanopore.

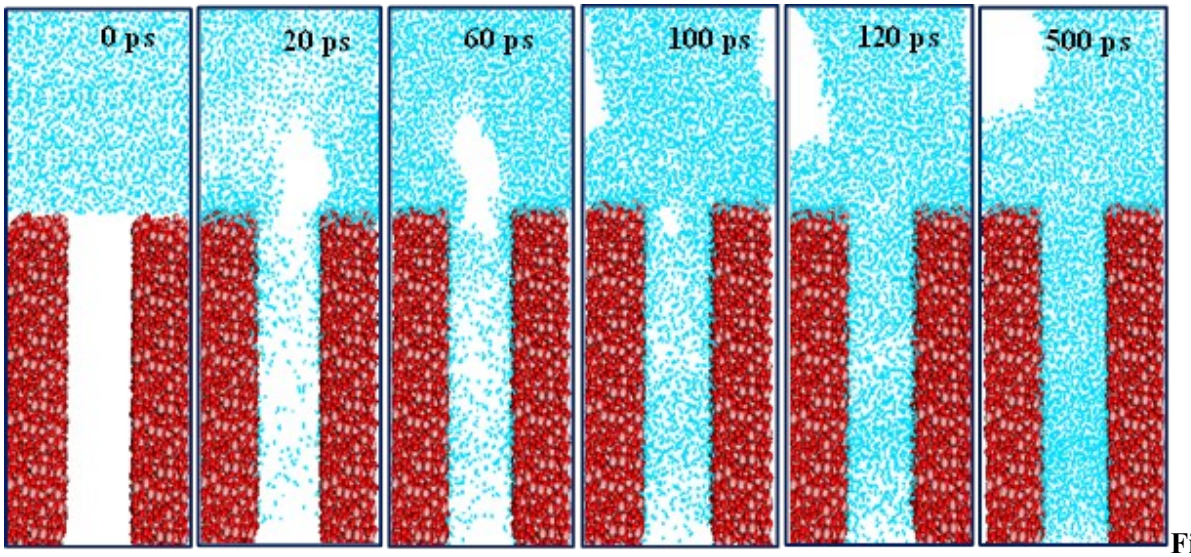


**Fig. S8** Representative MD simulation snapshots of water loading into a $TiO_2$ nanopore.

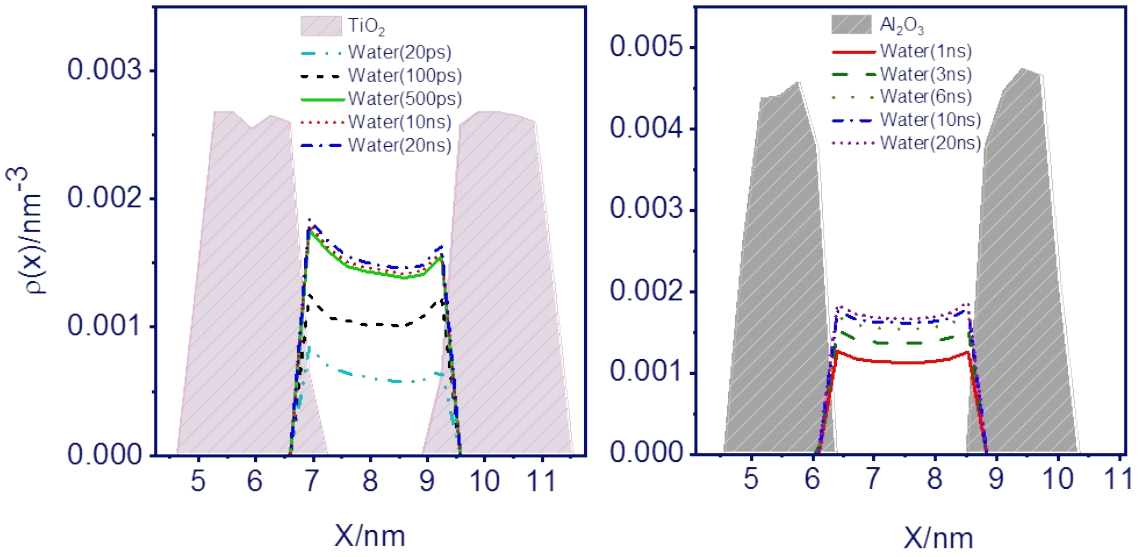


**Fig. S9** Calculated number of density profiles along the x-direction of water inside the $TiO_2$ and $Al_2O_3$ nanopores at different simulation times.

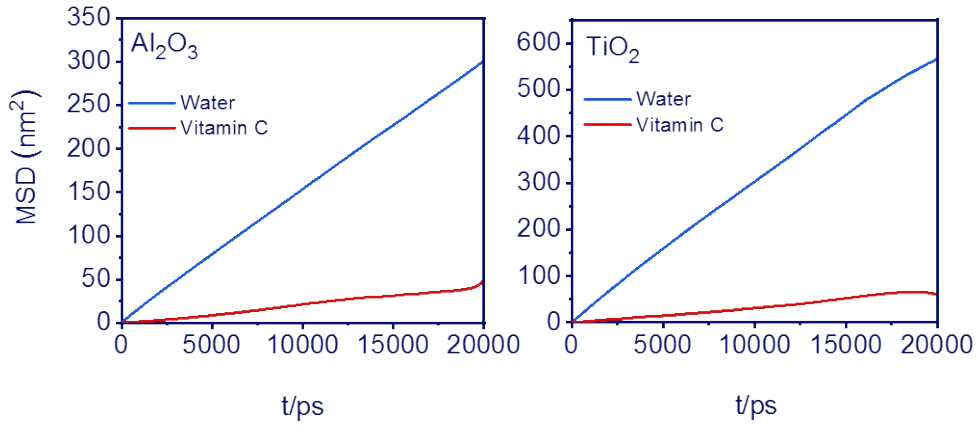


**Fig. S10** Calculated mean-square displacement of the geometrical centers of water and vitamin C for confined vitamin C solutions in the $Al_2O_3$ and $TiO_2$ nanopores.

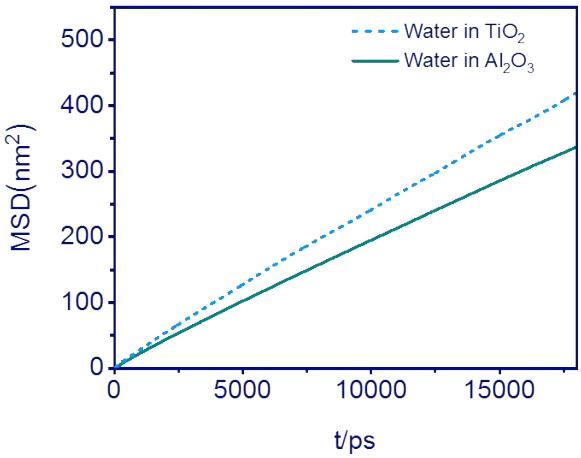


**Fig. S11** Calculated mean-square displacement of geometrical centers of confined pure water in the $Al_2O_3$ and $TiO_2$ nanopores.

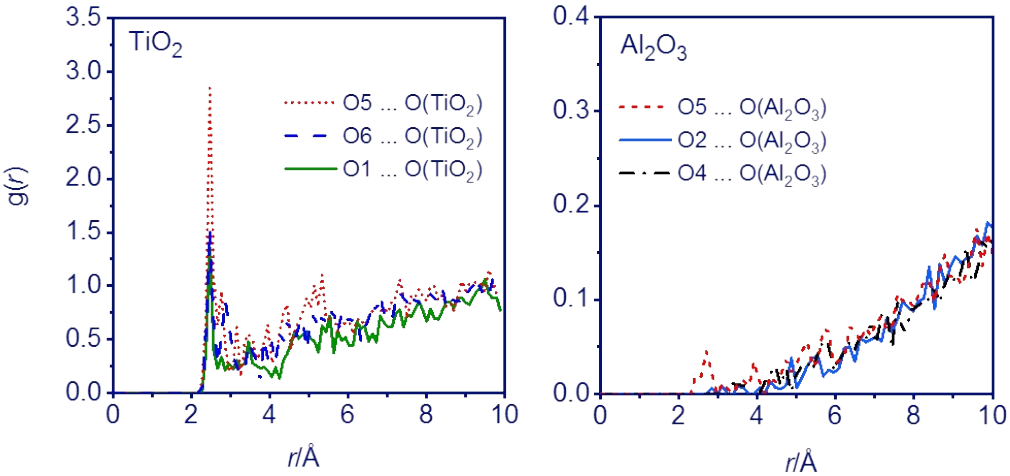


**Fig. S12** Calculated radial distribution functions g(*r*) of O atoms of vitamin C with O atoms of the $Al_2O_3$ and $TiO_2$ nanopores.

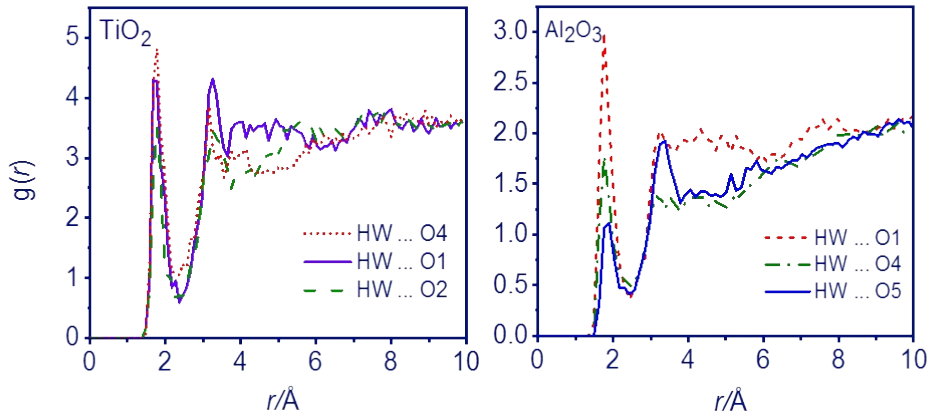


**Fig. S13** Calculated radial distribution functions g(*r*) of water H atoms with O atoms of vitamin C in the $Al_2O_3$ and $TiO_2$ nanopores.

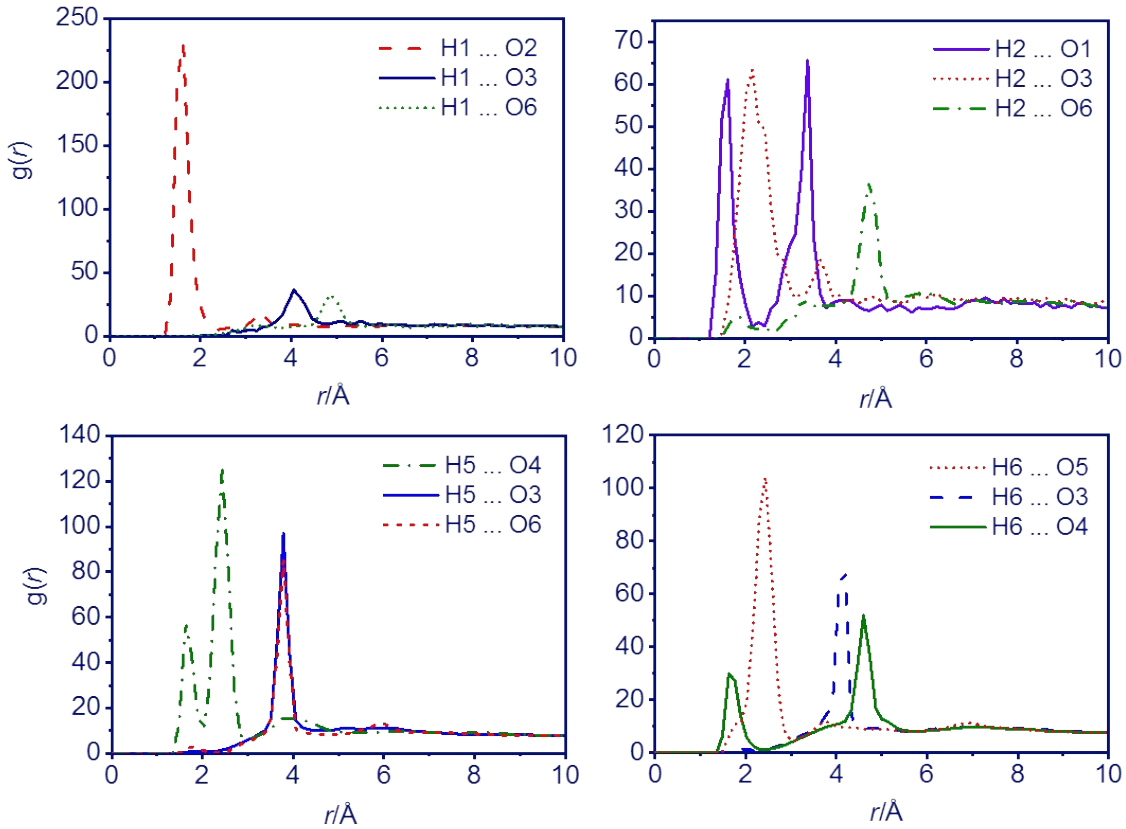


**Fig. S14** Calculated radial distribution functions g(*r*) between H atoms of a vitamin C molecule with O atoms of another vitamin C molecules in an $Al_2O_3$ nanopore.

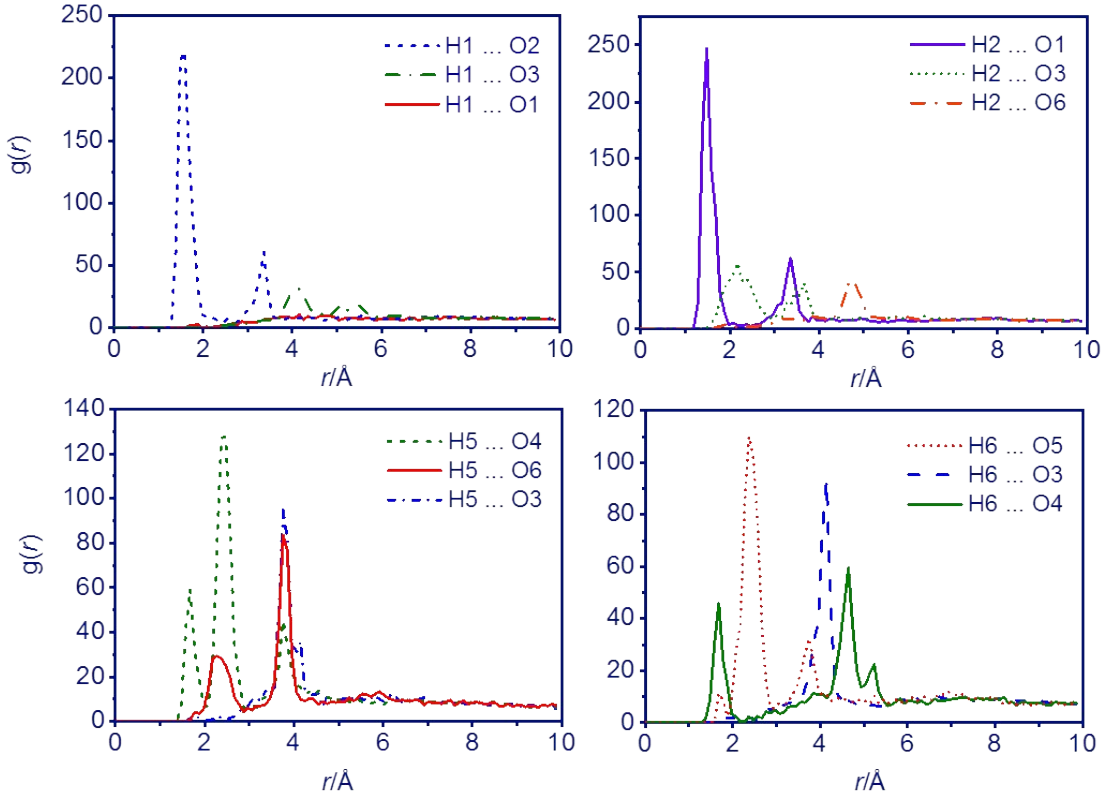


**Fig. S15** Calculated radial distribution functions g(*r*) of H atoms of a vitamin C molecule with O atoms of another vitamin C molecule in a $TiO_2$ nanopore.

**B) Supporting Tables**

**Table S1** DFT-calculated atomic charges for vitamin C

| atom | q/e<br>B3LYP<br>NBO |
|---|---|
| O1 | -0.750 |
| O2 | -0.738 |
| O3 | -0.543 |
| O4 | -0.588 |
| O5 | -0.683 |
| O6 | -0.664 |
| H1 | 0.468 |
| H2 | 0.478 |
| H5 | 0.494 |
| H6 | 0.490 |
| C1 | 0.292 |
| C2 | 0.281 |
| C3 | 0.300 |
| C4 | 0.749 |
| C5 | 0.117 |
| C6 | 0.297 |